Journal of Photochemistry and Photobiology A: Chemistry 207 (2009) 153–159

Contents lists available at ScienceDirect

Journal of Photochemistry and Photobiology A: Chemistry

journal homepage: www.elsevier.com/locate/jphotochem

Roles of H_2O_2 and $OH^\bullet$ radical in bactericidal action of immobilized TiO_2 thin-film reactor: An ESR study

Guoliang Yan [a], Jian Chen [b], Zhaozhe Hua [b,*]

[a] College of Food Science and Nutrition Engineering, China Agriculture University, Beijing 100083, PR China
[b] Key Laboratory of Industrial Biotechnology, Ministry of Education, Jiangnan University, 1800 Lihu Road, Wuxi 214122, PR China

ARTICLE INFO

Article history:
Received 26 May 2008
Received in revised form 12 January 2009
Accepted 3 March 2009
Available online 17 March 2009

Keywords:
Reactive oxygen species
Immobilized TiO_2 thin-film reactor
ESR spin-trapping
Photocatalytic bactericidal effect

ABSTRACT

To evaluate the bactericidal roles of hydrogen peroxide (H_2O_2) and hydroxyl radical ($OH^\bullet$) in immobilized titanium dioxide (TiO_2) thin-film reactor, the mechanism of H_2O_2 and $OH^\bullet$ formation in photocatalytic reaction was investigated by applying electron spin resonance (ESR) technique. The results showed that the formation of $OH^\bullet$ largely depended on H_2O_2 formed in photocatalytic reaction. $OH^\bullet$ were mainly originated from the H_2O_2 via the reduction reaction although a relatively small portion came from the direct photolysis of H_2O_2. Due to the convertible relationship between H_2O_2 and $OH^\bullet$, the approaches that can increase H_2O_2 concentration such as bubbling air or adding H_2O_2 could greatly result in enhancement of $OH^\bullet$. The results of bactericidal experiments showed that killing effect was completely inhibited by catalase, in contrast, the inactivation efficiency was proportionally increased with elevated H_2O_2 levels. Considering the fact that H_2O_2 alone was not enough to complete the disinfection action, it is concluded that $OH^\bullet$, not H_2O_2 was the primary bactericidal radicals in the immobilized TiO_2 thin-film reactor; however, due to its conversion to $OH^\bullet$ and oxidative toxicity, H_2O_2 was also indispensable for photocatalytic bactericidal effect.

1. Introduction

In 1985, Matsunaga et al. reported for the first time the antibacterial effect of TiO_2 photocatalytic reactions [1]. Since then, the biological effect of TiO_2 photocatalyst has attracted increasing attention worldwide because of its stable and strong oxidative reactions resulting in biocidal activity. It is generally accepted that the mechanism of cell death by the TiO_2 photochemical reaction involves photogenerated holes and reactive oxygen species (ROS) such as superoxide radical (O_2^-), hydrogen peroxide (H_2O_2) and hydroxyl radical ($OH^\bullet$). Mechanisms for the primary events occurring at the catalyst surface have been described [2,3]. Upon excitation by light whose wavelength is less than 385 nm, an electron (e^-) is promoted from the valence band to the conduction band of the semiconducting oxide leaving a positive hole (h^+) in the valence band. The positive hole can oxidize H_2O to $OH^\bullet$ (Eqs. (1) and (2)), and the negative electron can reduce oxygen to O_2^- or H_2O_2 in the presence of molecular oxygen (Eqs. (3) and (4)).

$$TiO_2 \rightarrow TiO_2(e^- + h^+) \quad (1)$$

$$H_2O + h^+ \xrightarrow{TiO_2} HO^\bullet + H^+ \quad (2)$$

$$O_2 + e^- \xrightarrow{TiO_2} O_2^- \quad (3)$$

$$O_2^- + e^- + 2H^+ \rightarrow H_2O_2 \quad (4)$$

The photogenerated H_2O_2 and O_2^- will then promote the generation of $OH^\bullet$ in TiO_2 photocatalytic reactor (Eqs. (5) and (6)).

$$H_2O_2 + e^- \rightarrow OH^\bullet + OH^- \quad (5)$$

$$H_2O_2 + O_2^- \rightarrow OH^\bullet + OH^- + O_2 \quad (6)$$

In addition, $OH^\bullet$ can be formed from the photolytic decomposition of H_2O_2 by the UV illumination (Eq. (7)), especially UV electromagnetic spectrum between 200 and 280 nm [4].

$$H_2O_2 \xrightarrow{h\nu} 2OH^\bullet \quad (7)$$

On the other hand, H_2O_2 can react with $OH^\bullet$ and h^+ to form the hydroperoxyl radical ($HO_2^\bullet$), especially when the concentration of H_2O_2 is high (Eqs. (8) and (9)), which can reduce the concentration of $OH^\bullet$ (5).

$$H_2O_2 + OH^\bullet \rightarrow HO_2^\bullet + H_2O \quad (8)$$

$$H_2O_2 + h^+ \rightarrow HO_2^\bullet + H^+ \quad (9)$$

The TiO_2 may be used either as an aqueous slurry or be immobilized onto a supporting substrate. When titania suspensions are used, the catalyst must be recovered at the end of the treatment, either by filtration or sedimentation which is expensive in terms

* Corresponding author. Tel.: +86 510 85918309; fax: +86 510 85918309.
E-mail address: huazz@jiangnan.edu.cn (Z. Hua).

1010-6030/$ – see front matter © 2009 Elsevier B.V. All rights reserved.
doi:10.1016/j.jphotochem.2009.03.003

of time, reagents and manpower. Alternatively, the TiO_2 can be immobilized onto a supporting substrate such as glass to avoid catalyst-recovering step [6]. Among the immobilized reactors, the immobilized TiO_2 thin-film reactors appear to be the most promising in terms of practical applications [7]. A thin-film catalyst can be prepared using a sol–gel technique and the supporting substrate coated with thin-film TiO_2 can be mounted in a reactor or be positioned outside of UV lamp to receive UV irradiation for the inactivation of cell.

It is clear that an in-depth understanding of the reaction mechanism responsible for photocatalytic inactivation of cells is helpful to increase the efficiency of photocatalytic disinfection system and devise a strategy in a practical system to efficiently kill microorganisms. However, there still exists controversy regarding the major species which is responsible for the photocatalytic bactericidal effect. It is frequently assumed that $OH^•$ are the main oxidative species responsible for the photocatalytic inactivation of bacteria [8–10]. Ireland et al. [8] reported that no inactivation of *E. coli* in the presence of the $OH^•$ scavenger was observed. The results of Sjogren and Sierka [9] showed that a 200% enhancement of its inactivation in the presence of a low concentration of ferrous ions. This observation of enhanced MS-2 phage inactivation was explained by the increased $OH^•$ concentration resulting from the Fenton reaction, as well as from the photocatalytic reaction ($Fe^{2+} + H_2O_2 — Fe^{3+} + OH^- + OH^•$, $Fe^{3+} + e^- — Fe^{2+}$). However, there is also some evidence that H_2O_2 contribute to the photocatalytic inactivation of cells. For example, Kikuchi et al. [11] proposed that the main bactericidal source is not the $OH^•$, but H_2O_2 in *E. coli* suspension separated from the TiO_2 thin film, since catalase that can decompose H_2O_2 greatly hindered the inactivation of *E. coli*, whereas the $OH^•$ scavenger did not. Maness et al. [12] reported that H_2O_2 and O_2^-, as well as the $OH^•$, play significant role in microorganism inactivation. In these studies, the authors generally applied ROS scavengers such as mannitol and catalase or catalysts such as Fe^{2+} to validate their assumption, but seldom check the formations of ROS, especially the $OH^•$. Obviously, monitoring ROS generation in photocatalytic reaction can provide direct evidence for identifying the primary bactericidal ROS. ESR spin-trapping technique appears to be one of the promising approaches for the detection of radicals' production, which has been used to observe directly ROS generate in TiO_2 photocatalytic reactor and provides essential information for understanding of the reaction mechanism on semiconductor surfaces [13,14]. In this work, to evaluate the bactericidal roles of H_2O_2 and $OH^•$ in immobilized TiO_2 thin-film reactor, the ESR spin-trapping technique using 5,5-dimethyl-1-pyrroline-*N*-oxide (DMPO) as spin trap was applied to investigate the reaction mechanism of H_2O_2 and $OH^•$ in photocatalytic reaction. The bactericidal experiments were further performed using *Bacillus* sp. F26 as a model bacterium. The effects of O_2 and H_2O_2 on photocatalytic bactericidal efficiency were investigated.

2. Materials and methods

2.1. Materials

The photocatalytic reactor used in the experiment was kindly provided by Professor Fumihide Shiraishi of Kyushu Institute of Technology (Japan). Photocatalyst was prepared according to the method reported by Shiraishi et al. [15] as follows: amorphous TiO_2, prepared from titanium isopropoxide, was dissolved into an aqueous solution of H_2O_2, which give a transparent yellow solution. After this solution was swabbed on the surface of a quartz glass tube of 140 mm long and 28 mm inside diameter, the glass tube was fired at 500 °C for 1 h, by which a transparent thin film of TiO_2 on quartz glass tube was formed. The spin trap reagent DMPO was purchased from Sigma (USA) and stored at −20 °C in a freezer. All solutions and reagents were prepared in deionized/distilled water, analytical reagent-grade chemicals were used (Aldrich, USA). All glassware used in these experiments was washed with distilled water, and then autoclaved at 121 °C for 15 min.

2.2. Experimental procedures

The reactions were carried out in an annular-flow photocatalytic reactor as illustrated in Fig. 1(A). The photocatalytic reactor was a cylindrical plastic vessel in which a 6.0 W UV lamp (254 nm), protected by a quartz glass tube from direct contact with the aqueous solution, was located at the center. Another big quartz glass tube with a membrane of TiO_2 on its outside wall was used as a sheath of the quartz glass. ROS were generated when the UV lamp was on and solution flowed through the space between the inner wall of the vessel and the glass sheath.

The photocatalytic reactor, a pyrex glass bottle (Vessel), a cooling apparatus, a flow meter and a peristaltic pump were connected in a loop, showed in Fig. 1(B). 350 mL deionized water was poured into the mixed-flow vessel (800 mL) and then recycled by means of a peristaltic pump at a flow rate of 300 mL/min. The reaction was started by switching the UV lamp on. At the same time, aseptic air was sparged into the pyrex glass bottle at the rate of 6 L/min. Operational conditions for all runs were kept at pH 7.0, temperature at 28.0 °C through a cooling apparatus. During the reaction, liquid sample was withdrawn at appropriate time intervals from the bottle and analyzed immediately by means of H_2O_2 quantification

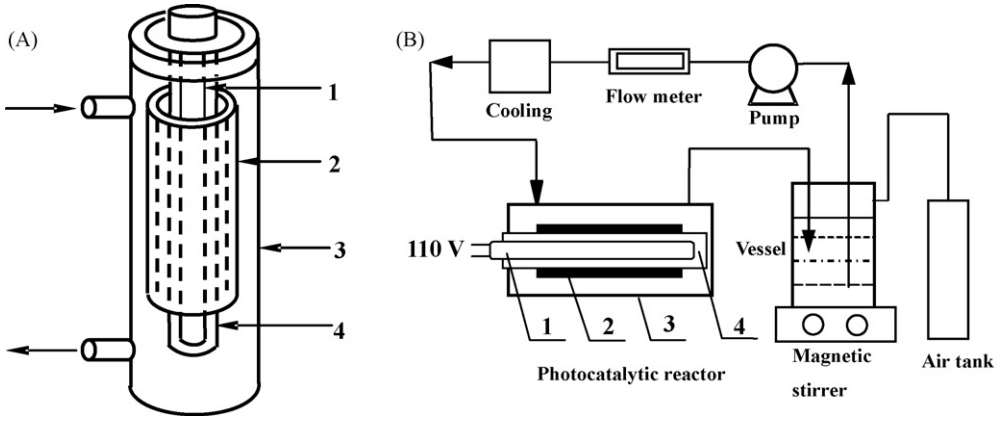

Fig. 1. Annular-flow photocatalytic reactor (A) and schematic diagram of experimental apparatus (B). (1) Ultraviolet lamp (6 W); (2) glass tube with photocatalyst membrane; (3) cylindrical plastic vessel (height: 20 cm, diameter: 5 cm); (4) quartz glass.

and ESR analysis described below. In the confirmation of $OH^{\bullet}$ and O_2^-, dimethyl sulphoxide (DMSO), superoxide dismutase (SOD) and catalase (CAT) were introduced into the pyrex glass bottle prior to UV illumination, respectively.

2.3. Analytical techniques

The ESR spectrometer was used to detect and monitor the free radicals generated in reactor. The spin trap reagent, DMPO was dissolved in deionized water under the deair condition full of nitrogen and separated in 1 mL cone test tubes before experiments. In order to improve the noisy baseline ESR spectrum, the deionized water was sparged with helium gas for 2 h to remove any oxygen dissolved in the water before adding DMPO. The 0.5 mL sample contained ROS taken from the mixed-flow vessel was introduced into the cone test tube and mixed with the DMPO solution for reaction. The final reaction volume was 0.8 mL and the concentration of DMPO is 0.5 mM. The sample (100 μL) was immediately transferred into quartz capillaries specially designed for ESR analysis after 30 s for reaction and ESR spectra were recorded with a Bruker EMX 10/12 spectrometer at room temperature. ESR measurements were conducted under the following conditions: centre field, 3480 G; sweep width, 200 G; microwave frequency, 9.766 GHz; microwave power, 20.0 mW; modulation frequency, 100 KHz; modulation amplitude, 3.0 G; scan, 84 s; time constant, 41.0 ms. number of scans, 5.

The H_2O_2 concentrations produced in photocatalytic reactor were determined according to the enzymatic method described by Shiraishi et al. [16].

2.4. Disinfection experiments

In order to evaluate bactericidal effects of H_2O_2 and $OH^{\bullet}$, *Bacillus* sp. F26, isolated from Haoji Soda Lake located in the Hulunbeir area of Inner Mongolia Autonomous Region (China) was used as the model microorganism [17]. Our previous study showed that the strain is highly resistant to the oxidative stress [18]. The photokilling experiments were conducted as follows: *Bacillus* sp. F26 was cultivated aerobically at 37 °C with continuous shaking at 200 rpm in modified Horikoshi I medium containing (per liter of distilled water) 10 g of glucose, 10 g of polypeptone (BBI), 5 g of yeast extract (Oxoid), 1 g of KH_2PO_4, 0.2 g of $MgCl_2$, 50 g of NaCl, and 10 g of Na_2CO_3. To ensure synchronous growth, 20 h-old culture was inoculated into the fresh medium and cultivated for 16 h to its exponential phase. The cells were harvested at this stage and used in the experiments. Bacterial cells were collected by centrifugation at 500 × *g* for 10 min at 4 °C and the bacterial pellet was washed three times with deionized water. The cells were re-suspended and diluted to 10^7–10^8 colony forming units (CFU)/mL with sterilized water. Cell suspensions were diluted with sterilized water in the pyrex glass bottle to the required cell density corresponding to 10^5–10^6 CFU/mL. The experiment subsequently began when the UV lamp was switched on and performed for 100 min at room temperature. Samples were taken at 20 min interval, diluted in 50 mM potassium phosphate buffer and plated on the cultured medium agar plates in triplicate. The number of colonies appearing on the plates after 24 h of incubation at 37 °C was counted in terms of CFU.

3. Results and discussion

3.1. Generation of H_2O_2 in TiO_2/UV thin-film photocatalytic reactor

Fig. 2 illustrates the time-course of H_2O_2 produced in photocatalytic reactor. It could be seen that the concentration of H_2O_2 increased with the illuminated time prolonged and the maximum value (0.033 mM) appeared after 12 h of illumination, but further

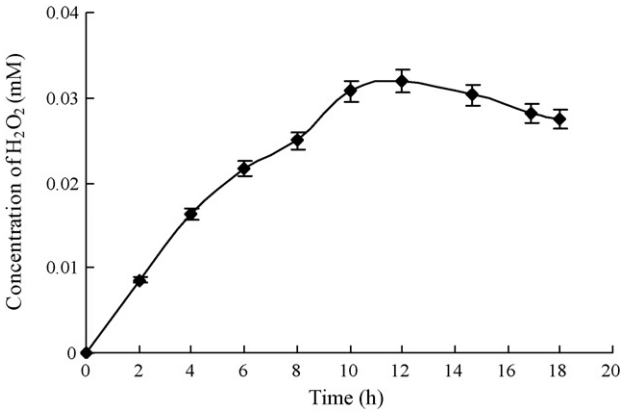

Fig. 2. Time-course of H_2O_2 concentration in TiO_2 thin-film reactor. Error bars indicate the S.D.

irradiation resulted in low concentration. According to Eqs. (1)–(4), H_2O_2 is mainly generated from the reduction reaction of O_2 (Eq. (4)). Once formed, it would convert to $OH^{\bullet}$ through the further reduction (Eqs. (5) and (6)) and the photolysis (Eq. (7)). Meanwhile, H_2O_2 can also react with $OH^{\bullet}$ and h^+ to form the HO_2^- (Eqs. (8) and (9)), which could result in reduction of H_2O_2 concentration. However, according to the results of Bekbolet and Balcioglu [5] that the oxidation reaction of H_2O_2 was minor compared to the reduction reaction unless higher concentrations of H_2O_2 (above 10 mM) were present, in our case, it was believed that the contribution of oxidation reaction to H_2O_2 level decline was insignificant due to its low concentration. Our results suggested that the H_2O_2 generation from O_2 reduction was faster than H_2O_2 decomposition (Eqs. (5)–(7)) before 12 h of irradiation. After that, the latter exceeded the former.

3.2. ESR measurement of ROS generated in TiO_2/UV thin-film photocatalytic reactor

Fig. 3 presents the time-course of ESR spectra measured in photocatalytic reactor in the presence of DMPO as the spin trap. It could be observed that the intensities of signal strengthened with increased irradiation time, indicating the concentrations of free radicals increased with the irradiation time prolonged. The ESR spectrums are composed of a four-line signal, having a peak height ration of 1:2:2:1 signal pattern and hyperfine coupling constant ($\alpha_N = \alpha_H = 14.9$ G) matched with those of typical DMPO–OH adduct formed upon trapping of $OH^{\bullet}$ by the DMPO [19].

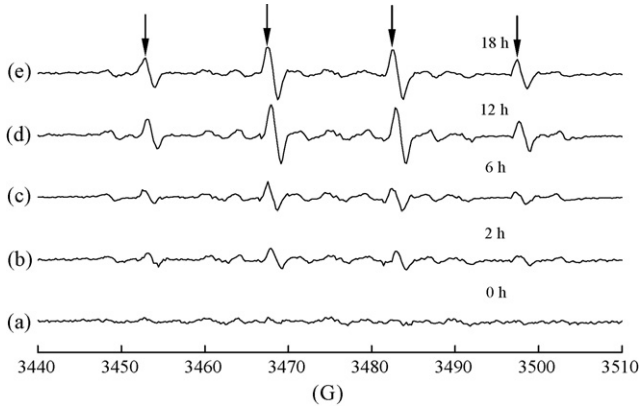

Fig. 3. ESR spectra of DMPO adducts measured in TiO_2 thin-film reactor. Spectra a–e denote the irradiation time 0, 2, 6, 12 and 18 h, respectively. (Arrow denotes the position of hyperfine peaks of DMPO–OH adducts).

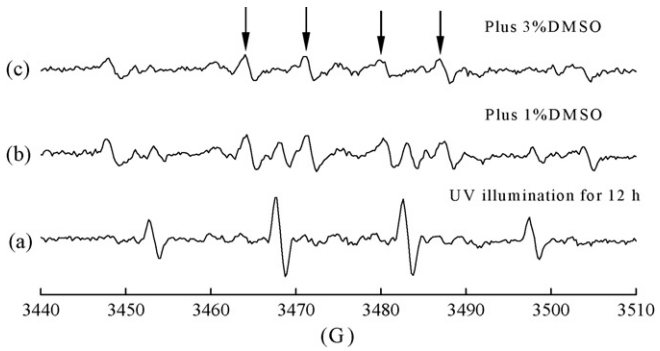

Fig. 4. ESR spectra of the DMPO adducts in 1% and 3% DMSO. (a) After 12 h of irradiation; (b) same as (a), except that 1% DMSO was added into the reactor prior to irradiation; (c) same as (a), except that 3% DMSO was added into the reactor prior to irradiation. (Arrow denotes the position of hyperfine peaks of DMPO–CH_3 adducts).

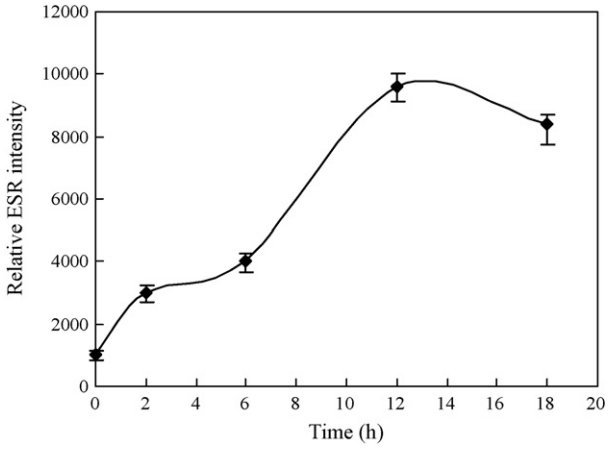

Fig. 5. Evolution of the DMPO–OH signal intensity (evaluated from the amplitude of the second line of the signal) as a function of the time of irradiation. Error bars indicate the S.D.

It should be pointed out that the observed increase in the DMPO–OH signals may be due to the decay of the O_2^- adduct, DMPO–OOH, or from a combination of both process. Therefore, 1% and 3% DMSO were pre-added into the reactor (Fig. 4). DMSO can react with OH• to give CH_3 radicals which can react with DMPO to yield DMPO–CH_3 with its characteristic hyperfine splitting pattern. The results showed that the signal of DMPO–OH decreased and disappeared in the presence of 1% and 3% DMSO, respectively, but presented features corresponding to the DMPO–CH_3 adduct (α_N = 16.4 G, α_H = 23.3 G) [20]. This suggests that the DMPO–OH signal observed in the absence of DMSO originated from the trapping of OH• and not from the decomposition of DMPO–OOH. Further evidence for the source of the DMPO–OH signal was obtained by carrying out the reaction in the presence of SOD (40 μg/mL), which can catalytically convert the O_2^- to H_2O_2 and O_2. It was found that the signal of OH• adducts were insensitive to SOD and inactivated SOD (date not shown). The similar phenomena were observed in the samples after illuminated for 2, 6 and 18 h (date not shown), suggesting that the intensities of ESR spectrums in Fig. 3 were induced by OH• adducts.

Although O_2^- should be formed as a result of the scavenging of the electron by O_2, we were unable to detect directly the spin-adduct of this radical under the present condition. Similar results were reported by other authors [21–23]. This may be due to the fact that O_2^- in water is very unstable and undergo facile disproportionation rather than slow reaction with DMPO [21]. Alternatively, it can be explained by the assumption that O_2^- is not desorbed or that it reacts quickly towards other products (e.g., H_2O_2) [23]. In fact, the role of O_2^- in photocatalytic disinfection was demonstrated to be insignificant relative to H_2O_2 and OH•. For example, the results of Cai et al. showed that antibacterial efficiency greatly increased in the presence of SOD and Fenton reagent due to the formation of H_2O_2 and OH• from O_2^- [24].

To determine the relative levels of OH• formed in photocatalytic reaction, evolution of the DMPO–OH• signal intensity as a function of irradiation time is presented in Fig. 5, which were evaluated from the amplitude of the second line of the signal [25]. It showed that like the profile of H_2O_2, the intensity of DMPO–OH adduct gradually enhanced with illumination time increased and reached the peak at 12 h, after that, began to decline. Similar results were reported by Brezova et al. [26]. These results suggested that the production of H_2O_2 can promote the generation of OH•. With regard to the decrease of DMPO–OH• signal intensity by prolong irradiation, it might be due to the multiple addition of OH• to DMPO, producing ESR-silent products [26].

3.3. The transformation of H_2O_2 into OH•

Numerous studies have demonstrated that there is a good correlation between the photocatalytic bactericidal efficiency and the amount of OH•. Therefore, it is important to clarify the originating source of OH• in photocatalytic reaction to improve the efficiency of photocatalytic sterilization. According to Eqs. (1)–(7), OH• are

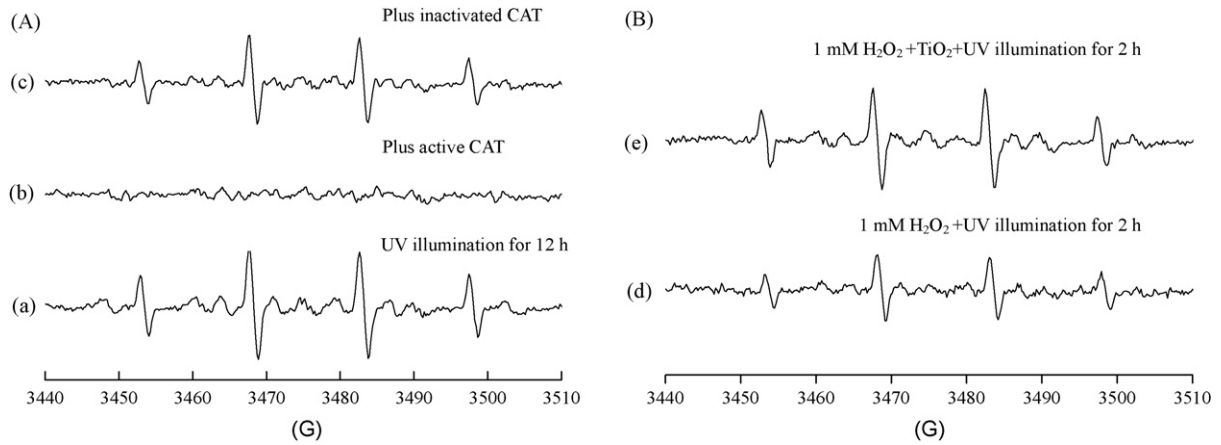

Fig. 6. ESR spectra of the DMPO adduct in CAT (A) and exogenous H_2O_2 without and with TiO_2 (B). (a) After 12 h of irradiation; (b) same as (a), except that active CAT (4 mg/mL) was added prior to irradiation; (c) same as (a), except that inactivated CAT (by heat) was added prior to irradiation; (d) 1 mM H_2O_2 was irradiated for 2 h in the absence of TiO_2; (e) 1 mM H_2O_2 was irradiated for 2 h in the presence of TiO_2.

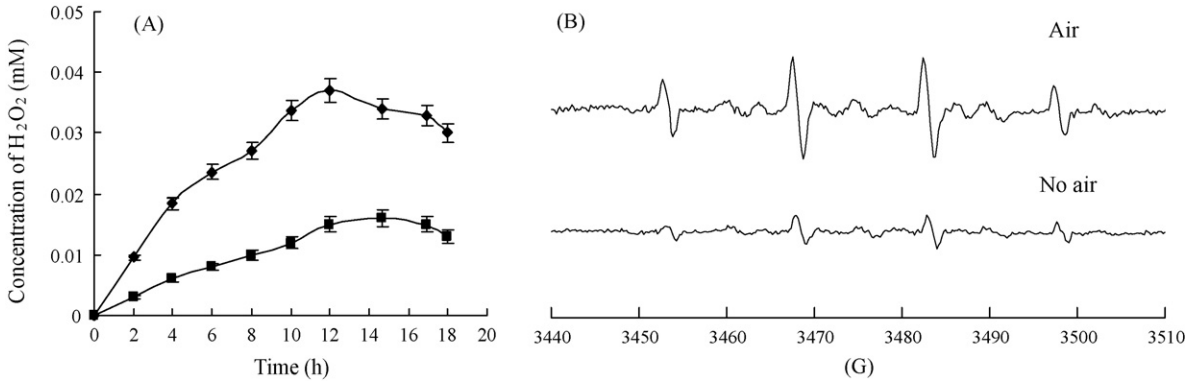

Fig. 7. Comparisons of H_2O_2 concentration (A) and ESR spectra (B) with and without air. (♦) 10 L/min of air was introduced into the vessel in the presence of UV illumination and TiO_2; (■) no air was introduced into the vessel. The ESR spectra of DMPO adduct were obtained after 12 h illumination. Error bars indicate the S.D.

produced from the following three routes: (1) reaction of positive hole (h^+) with H_2O (Eq. (2)); (2) the reduction reaction of H_2O_2 with electron (Eqs. (5) and (6)) and (3) direct decomposition of H_2O_2 by UV light (Eq. (7)), especially UV spectrum is located between 200 and 280 nm [4]. To elucidate which pathway among pathway 1–3 is the main route to the OH• formation, ESR experiments were performed in the presence of catalase (CAT), which catalytically converts the H_2O_2 to H_2O and O_2. As showed in Fig. 6A, the signals of DMPO–OH adduct disappeared after addition of active CAT (4 mg/mL), but the inactivated CAT did not produce similar results. Obviously, H_2O_2 is indispensable for the formation of OH•. OH• may either come from the H_2O_2 reduction or from direct photolysis, or a combination of both pathways. The ESR experiment was further carried out to identify which is the primary route. To strengthen the signal of ESR spectra for easy comparison, 1 mM H_2O_2 was added into the reactor with TiO_2 (H_2O_2/UV/TiO_2) and without TiO_2 (UV/H_2O_2) prior to UV illumination, respectively. The discrepancies in the ESR spectra were compared after 2 h of irradiation (Fig. 6B). In addition, the remained H_2O_2 concentration was measured.

It was obvious that the intensities of OH• adducts signal in UV/H_2O_2 decreased when TiO_2 film was removed. With regard to H_2O_2, its level dropped by about 28.1% in UV/H_2O_2 over the 120 min experiment time. In contrast, its level in the H_2O_2/UV/TiO_2 declined much more steeply with a 76.3% decrease after 120 min. These results indicated that TiO_2 could speed up the conversion of H_2O_2 to OH• and OH• were mainly originated from the H_2O_2 reduction. Previous studies showed that addition of H_2O_2 could greatly increase the efficiency of UV disinfection as a result of elevation of OH• by H_2O_2 direct photolysis; however, it was proved that its inactivated efficiency was lower compared with H_2O_2/UV/TiO_2 [27]. Our results well supported this conclusion.

Previous studies have showed that the introduction of pure oxygen or air can enhance the generation of H_2O_2• [28]. To evaluate the effect of endogenous H_2O_2 on the formation of OH•, the influences of air bubble (10 L/min and void air) on the formations of H_2O_2 and ESR spectra were investigated. As expected, the rate of H_2O_2 formed was accelerated by bubbling 10 L/min air and accordingly the maximum concentration increased by 131.2% when compared to those without air (Fig. 7A), the highest value of H_2O_2 was also 16.7% higher than the value obtained in 6 L/min (Fig. 2). Similarly, the intensity of DMPO adducts was enhanced by air bubble relative to that without air (Fig. 7B). This suggested that increased O_2 provided by air bubbles react with the electron trapped on the surface of TiO_2 and generate O_2^-. It further reacts with electron and form H_2O_2 (Eq. (4)), which then decomposed and produces OH• [3].

It is well known that the formation and transformation of oxygen radicals in photocatalytic reaction are dependent on their potential for oxygen reduction. Due to the truth that the potential for O_2 reduction is −0.13 V while that of H_2O_2 reduction is 0.72 V, H_2O_2 is a better electron acceptor than oxygen. This means that once H_2O_2 appear, the most electrons excited from band will turn to H_2O_2 for producing OH• instead of reacting with O_2 to form O_2^-. As a result, the accumulation of H_2O_2 was always accompanied by increase of OH• (Figs. 2 and 5). On the other hand, the failure of detecting O_2^- in this study could be explained by the assumption that the amount of O_2^- in reactor could not reach the level that efficiently trapped by DMPO due to the presence of H_2O_2.

In our study, it was found that the signal of DMPO–OH adduct was not immediately disappear after turn-off of the UV light, instead, it decayed much slowly and could be still observed after 20 min in the dark, implying that the photocatalytic reaction can continue to take place in the dark and lead to the OH• formation (Fig. 8). The similar results were reported by Liu et al. [22]. In photocatalytic inactivation study, it was also found that cells continue to lose their viability even after stop UV irradiation, which was called residual disinfection [29]. Maness et al. attributed it to the assumption that certain lethal reaction can continue to propagate after the UV illumination stops [12]. Another explanation is that oxidative species continue to generate and attack cellular membrane and probably enter into the cells leading to the bacterial cell death [30]. Our results in Fig. 8 seem to support the second assumption. Since the addition of CAT (4 mg/mL) resulted in disappearance of DMPO–OH adducts' signal after UV light was turned off (date not shown), it is assumed that OH• may come from the decomposition of H_2O_2 formed in the photocatalytic reaction. The detailed mechanism need to be further investigated.

3.4. The important roles of H_2O_2 and OH• in the bactericidal effects of TiO_2/UV thin-film photocatalytic reactor

Our results showed that the levels of OH• and H_2O_2 synchronously enhanced with the illumination time increased as a result of conversion of H_2O_2 to OH• (Figs. 2 and 5). In order to

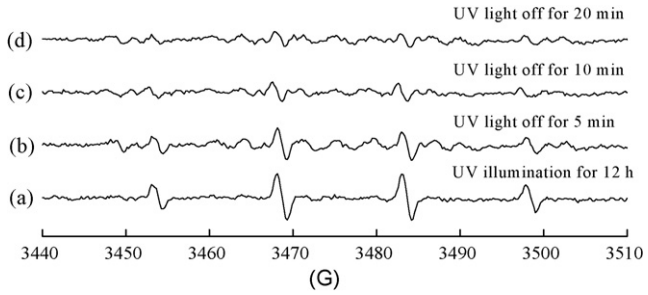

Fig. 8. Changes of DMPO adduct ESR spectra after UV light off. (a) After 12 h of irradiation; spectra b–d denote after 5, 10 and 20 min of UV light off, respectively.

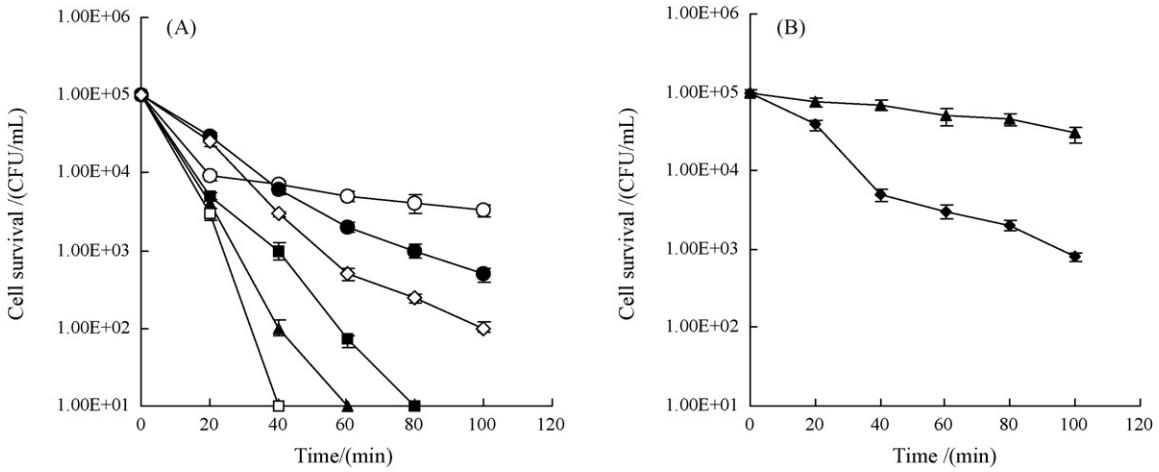

Fig. 9. Effects of air bubble and H_2O_2 (A) and catalase (B) on bactericidal efficiency of TiO_2 thin-film reactor. A: ● Control: 6 L/min of air was introduced into the vessel in the presence of UV illumination and TiO_2; ◊ Same as control, except that 10 L/min of air was introduced; ○ 6 mM H_2O_2 was added into the vessel without UV illumination; ■ Same as control, except that 1 mM H_2O_2 was added into the vessel prior to irradiation; ▲ Same as control, except that 3 mM H_2O_2 was pre-added; □ Same as control, except that 6 mM H_2O_2 was pre-added. B: ♦ Control: 6 L/min of air was introduced into the vessel in the presence of UV illumination and TiO_2; ▲ Same as control, except that CAT (4 mg/mL) was added into the vessel prior to irradiation. Error bars indicate the S.D.

determine their roles in killing effect, the bactericidal experiments were carried out using *Bacillus* sp. F26 as a mode microorganism. Considering the fact that UV lamp of 254 nm have germicidal effect, the control experiments were firstly conducted, in which TiO_2 film or UV light was removed from the photocatalytic reactor, respectively. The results showed that no obvious changes in bacteria survival in the absence of TiO_2 film or UV light, suggesting that disinfections without photocatalyst or in the dark were insignificant (data not shown).

Fig. 9A showed that the influences of bubbling air and H_2O_2 addition on photocatalytic killing effects. The bactericidal efficiency was enhanced by around 5-fold within 100 min of UV illumination in the 10 L/min air compared to the control (6 L/min), suggesting that increased H_2O_2 and OH• levels was induced by providing extra O_2. In contrast, increasing H_2O_2 concentration from 1 to 3 and finally to 6 mM resulted in a drastic inactivation effect, no viable cells were found after 40, 60 and 80 min irradiation in the presence of 6, 3, 1 mM H_2O_2. This suggests that a great amount of OH• was generated with the elevation of H_2O_2 through decomposition, and also indicates that H_2O_2 was more efficient than O_2 to increase bactericidal effect in TiO_2 film photocatalytic reactor due to its higher capability to react with electron [31]. It should be noted that H_2O_2 (6 mM) alone has the capability of killing cells. The survival number of cells decreased from 1×10^5 to 1×10^4 CFU/mL within 20 min, then after, the killing effect was negligible. This may be explained by the fact that H_2O_2 induced catalase production within *Bacillus* sp. F26 and therefore decomposed the remained H_2O_2 [18]. The above results indicated that OH•, not H_2O_2 was the major bactericidal radical in TiO_2 thin-film reactor. However, considering the convertible relationship between H_2O_2 and OH•, H_2O_2 was indispensable for photocatalytic bactericidal effect. To verify this assumption, H_2O_2 scavenger, CAT was added prior to illumination. As expected, no significant bactericidal effect was observed in the presence of 4 mg/mL CAT (Fig. 9B). This result also validated the conclusion from the control experiment that the germicidal effect of UV light alone was negligible, and the inactivation of *Bacillus* sp. F26 in TiO_2 thin-film reactor was attributed to ROS produced in the photocatalytic reaction.

Besides providing OH•, the possibility that H_2O_2 directly induce cells damage could not be precluded. It was proposed that the photokilling process consists of two steps [32]. The cell wall was initially attacked by OH•, followed by a progressive damage of the cytoplasmic membrane and intracellular components caused by other ROS attack, such as H_2O_2. Therefore, once the cells wall was broken or antioxidative systems were disrupted, H_2O_2 would easily enter into the cells to accelerate the cells death. In addition, when the membrane was perforated, Fe^{2+} and Cu^{2+} could be freely released into the environment and react with H_2O_2 to form OH•, result in aggravation of cell damage [3]. Our results in Fig. 9A validated the hypothesis, in that no discrepancy in cells number before 20 min in the presence of 1, 3, 6 mM H_2O_2 was observed, whereas, the rates of cell death were speeded up after 20 min with the H_2O_2 concentration elevated. On the basis of these results, it can be concluded that it is a cooperative work of OH• and H_2O_2 to complete the bactericidal process, in which OH• was the primary bactericidal oxygen radicals, and H_2O_2 as a supplier of OH• and another important attack radicals was also indispensable for disinfection effect.

4. Conclusions

In this study, the mechanism of H_2O_2 and OH• formation and transformation in the immobilized TiO_2 thin-film reactor was investigated by applying ESR spin-trapping technique. The results showed that the level of OH• was well associated with the amount of H_2O_2 because OH• was mainly originated from the H_2O_2 via the reduction reaction although a relatively small portion came from the direct photolysis of H_2O_2. The bactericidal efficiency of reactor was proportionally increased with elevated H_2O_2 levels, whereas, H_2O_2 alone was not enough to complete the disinfection action. Based on these results, it is concluded that OH•, not H_2O_2 was the primary bactericidal radicals in TiO_2 thin-film reactor; however, due to its conversion to OH• and oxidative toxicity, H_2O_2 was also indispensable for photocatalytic bactericidal effect.

Acknowledgements

This work was supported by a grant from the Major State Basic Research Development Program of China (973 Program) (No. 2007CB714306), Program for Changjiang Scholars and Innovative Research Team in University (IRT0532), and Program for New Century Excellent Talents in University, and program for Young Teacher in China Agricultural University. We also thanks Professor Fumihide Shiraishi of Kyushu Institute of Technology in Japan for his kindly providing the photocatalytic reactor used in the experiment.

References

[1] T. Mutsunaga, R. Tomodam, T. Nakajima, H. Wake, FEMS Microb. Lett. 29 (1985) 211.
[2] M. Bekbolet, F. Cecen, G. Ozkosemen, Water Sci. Tech. 34 (1996) 65.
[3] A.K. Benabbou, Z. Derriche, C. Felix, P. Lejeune, C. Guillard, App. Catal. B: Environ. 76 (2007) 257.
[4] S. Parsons, Advanced Oxidation Processes for Water and Wastewater Treatment, IWA Publishing, Cornwall, UK, 2004.
[5] M. Bekbolet, I. Balcioglu, Water Sci. Tech. 34 (1996) 73.
[6] T.A. McMurray, J.A. Byrne, P.S.M. Dunlop, J.G.M. Winkelman, B.R. Eggins, E.T. McAdamsa, Appl. Catal. A: Gen. 262 (2004) 105.
[7] D.H. Kim, M.A. Anderson, Environ. Sci. Technol. 28 (1994) 479.
[8] J.C. Ireland, P. Klostermann, E.W. Rice, R.M. Clark, Appl. Environ. Microbiol. 59 (1993) 1668.
[9] J.C. Sjogren, R.A. Sierka, Appl. Environ. Microbiol. 60 (1994) 344.
[10] M. Cho, H. Chung, W. Choi, J. Yoon, Water Res. 38 (2004) 1069.
[11] Y. Kikuchi, K. Sunada, T. Iyoda, K. Hashimoto, A. Fujishima, J. Photochem. Photobiol. A: Chem. 106 (1997) 51.
[12] P.C. Maness, S. Smolinski, D.M. Blake, Z. Huang, E.J. Wolfrum, W.A. Jacoby, Appl. Environ. Microbiol. 65 (1999) 4094.
[13] V. Brezova, S. Gabcova, D. Dvoranova, A. Stasko, J. Photochem. Photobiol. B 79 (2005) 121.
[14] R. Morelli, I.R. Bellobono, C.M. Chiodaroli, S. Alborghetti, J. Photochem. Photobiol. A 112 (1998) 271.
[15] F. Shiraishi, K. Toyoda, S. Fukinbara, Chem. Eng. Sci. 54 (1999) 1547.
[16] F. Shiraishi, T. Nakasako, Z.Z. Hua, J. Phys. Chem. A 107 (2003) 11072.
[17] W.Z. Zhang, Y.F. Xue, Y.H. Ma, W.D. Grant, A. Ventosa, P.J. Zhou, Extremophiles 6 (2002) 33.
[18] G.L. Yan, Z.Z. Hua, G.C. Du, J. Chen, Curr. Microbiol. 52 (2006) 238.
[19] H. Masaki, H. Sakurai, J. Dermatol. Sci. 14 (1997) 207.
[20] E. Finkelstein, G.M. Rosen, E.J. Rauckman, Arch. Biochem. Biophys. 200 (1980) 1.
[21] W.H. Ma, Y.P. Huang, J. Li, M.M. Cheng, W.J. Song, J.C. Zhao, Chem. Commun. 13 (2003) 1582.
[22] G.M. Liu, J.C. Zhao, H.J. Hidakab, J. Photochem. Photobiol. A: Chem. 133 (2000) 83.
[23] E.M. Ceresa, J. Mater. Sci. 18 (1983) 289.
[24] R. Cai, K. Hashimoto, A. Fujishima, Chem. Lett. 3 (1992) 427.
[25] M.D.H. Alonso, A.B. Hungria, A.M. Arias, M.F. Garcia, Appl. Catal. B: Environ. 50 (2004) 167.
[26] V. Brezova, D. Dvoranova, A. Stasko, Res. Chem. Intermed. 33 (2007) 251.
[27] A. Paleologou, H. Marakas, N.P. Xekoukoulotakis, A. Moya, Y. Vergara, N. Kalogerakis, P. Gikas, D. Mantzavinos, Catal. Today 129 (2007) 136.
[28] J.K. Kim, H.S. Choi, E. Kim, Y.S. Lee, Y.H. Kim, S.W. Kim, Biotechnol. Lett. 24 (2002) 1397.
[29] A.G. Rincón, C. Pulgarin, Appl. Catal. B: Environ. 49 (2004) 99.
[30] Z. Huang, P.C. Maness, D. Blake, J. Photochem. Photobiol. A: Chem. 130 (2000) 163.
[31] D.F. Ollis, E. Pelizzetti, N. Serpone, Environ. Sci. Technol. 25 (1991) 1523.
[32] S. Kayano, T. Watanabe, K. Hashimoto, J. Photochem. Photobiol. A: Chem. 156 (2003) 227.